Preprints of the 21st IFAC World Congress (Virtual)
Berlin, Germany, July 12-17, 2020

Adaptive control for systems with two binary measurements

Sebastian Leonow * **Martin Mönnigmann** **

* *Ruhr-Universität Bochum, Bochum, 44801 Germany (e-mail: sebastian.leonow@rub.de).*
** *Ruhr-Universität Bochum, Bochum, 44801 Germany (e-mail: martin.moennigmann@rub.de).*

Abstract: We propose a new type of binary controller for control loops with two binary measurements and an analog, continuous actuator. Unlike common binary controllers, the proposed adaptive controller requires no continued oscillation of the plant output. Instead, the proposed controller adapts an internal plant model to compute an optimal plant input so that the plant output settles on a constant value in between the two binary sensors. The parameter identification is fully automated and requires no user interaction, so that the proposed controller is as simple to implement as a conventional on-off controller. We evaluate the controller in a laboratory test setup and compare the energy comsumption to established control approaches.

Keywords: Adaptive control, Process control, Control of switched systems, Discontinuous control, Hybrid and switched systems modeling

1. INTRODUCTION

Binary controllers are widely used in industrial and home automation and are known for their simplicity and their unique stabilizing capabilities. Binary control is one of the simplest and most well-established control variants, although certain aspects like stability of binary control loops or the choice of optimal relay parameters are still subject to current research. Fundamental results exist on the stability of a binary control loop, e.g. by Åström (1959), Goncalves et al. (2001) and Goncalves et al. (2003). More recent results focus on specific system classes as in Colombo et al. (2007) or Co (2010) to obtain more general results for the regarded system class. Patents (e.g. Bek and Dietzel (1996)) and safety critical applications (e.g. in Yoon and Johnson (2017)) underline the industrial relevance of binary controllers.

While conventional binary controllers are typically simple on-off controllers, recent works propose to investigate the input and output signal ranges to obtain an increased control quality (e.g. Hetel et al. (2015), Afram (2016)) and also to investigate the influence of on-off controllers on the energy consumption of the controlled plant (e.g. Ahmad (2019), Cetin et al. (2019)). Besides an increased energy consumption, a major drawback of conventional on-off control is the high stress on the control loop components, in particular on the actuator. The widespread use of on-off controllers in HVAC and water pumping applications leads to a significant potential for optimization. In Leonow and Mönnigmann (2019) we proposed a new type of adaptive binary controller that is able to provide a much smoother control. The controller acts on a continuous actuator but still uses the simple and affordable binary measurement. In Leonow et al. (2019) we proposed an improved variant of the adaptive controller tailored for hydraulic applications, allowing for a quicker convergence towards the optimal parameters by adapting an internal plant model.

Here we further extend the adaptive binary controller to systems that feature two binary measurements. Our research is motivated by the observation that industrial devices are often equipped with limit switches for lower and upper bounds (cf. Fig. 1). While all other binary control concepts known to the authors perform a continued switching of the binary sensors to not lose the information about the process, the proposed adaptive controller converges towards a constant control output, comparable e.g. to a continuous PID control. The proposed controller is self-learning and requires no parameter tuning by the user. In the sample process in Fig. 1, the proposed controller could achieve a constant fluid level centred between the two float switches, without requiring information besides the two binary measurements. A PID controller could obviously achieve the same control quality, but would require tuning and a more elaborate, continuous measurement of the fluid level, both of which are expensive.

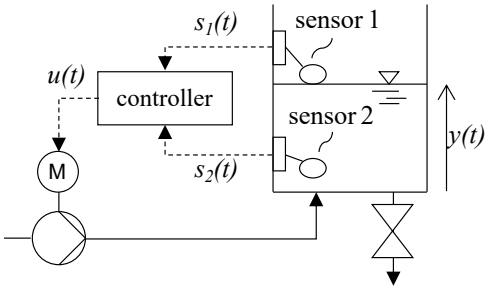

Fig. 1. Storage tank control with a variable speed pump and two float switches.

We organized the paper as follows: Section 2 introduces the regarded system class and the notation. Section 3 outlines the computation of the optimal controller parameters, while section 4 focuses on the controller algorithm. Section 5 gives results on the adaptive binary controller from a laboratory test setup.

2. PRELIMINARIES

The controlled plant is assumed to have a first order behaviour

$$T\dot{y}(t) = -y(t) + k(t)u(t) + z(t) \tag{1}$$

with $T > 0$. The plant input is assumed to be bounded to $u(t) \in [\underline{u}, \overline{u}]$ with $0 \leq \underline{u} < \overline{u}$. We assume that the plant gain $k(t) > 0$ and the output disturbance $z(t)$ change slowly compared to the time constant T and that the plant allows to be controlled by a conventional on-off controller.

Let the plant have two binary sensors that transform the process variable $y(t)$ into binary measurements $s(t) \in \{0, 1\}$ by

$$s_i(t) = \begin{cases} 1 : (y(t) > w_i + h_i) \vee (y(t) > w_i - h_i \wedge s_i(t-) = 1) \\ 0 : (y(t) < w_i - h_i) \vee (y(t) < w_i + h_i \wedge s_i(t-) = 0), \end{cases} \tag{2}$$

where $w_1 < w_2$ and $h_1, h_2 \geq 0$ as depicted in Fig. 2. The sensor setpoints w_i as well as the hystereses h_i are considered to be unknown but constant. We denote the outer bounds of the measurement range covered by the sensors by $\underline{y} = w_1 - h_1$ and $\overline{y} = w_2 + h_2$ and the overall hysteresis span by $H = \overline{y} - \underline{y}$.

The binary controller closes the control loop by generating a plant input $u(t)$ according to the sensor outputs $s_i(t)$:

$$u(t) = \begin{cases} \mu + \gamma\delta & , \; s_1(t) \vee s_2(t) = 0 \\ \mu - \gamma\delta & , \; s_1(t) \wedge s_2(t) = 1 \\ u(t-) & , \; \text{otherwise} \end{cases}, \tag{3}$$

where $u(t) = u(t-)$ means that the controller holds the current value of $u(t)$. The binary parameter $\gamma \in \{0, 1\}$ is initially set to 1 and will be further explained in section 4. We define a feasible controller by a set of parameters μ and δ that fulfill $\underline{y} > k(\mu - \delta)$ and $\overline{y} < k(\mu + \delta)$, i.e. the controller is able to apply inputs $u(t)$ large enough to reach the switching points of the binary sensors.

We assume all model and sensor parameters to be unknown and will outline in the following section 3 how to derive the parameters required to set up the binary controller parameters μ and δ in an automated algorithm that requires no interaction by the user.

3. OPTIMAL CONTROLLER PARAMETERS

Let the optimal controller parameters μ^* and δ^* be defined by the following rules:

- $u(t) = \mu^*$ yields $y(t) = y^* = 0.5(\underline{y} + \overline{y})$ and
- $u(t) = \mu^* \pm \delta^*$ yields $y^* \pm H$,

in an undisturbed, steady state case of the plant. In other words μ^* is the plant input required to achieve $y(t) = y^*$, i.e. centred between the two binary sensors, and $\pm\delta^*$ is the minimal amplitude that has to be added to μ^* to reach the sensor switching points at $\overline{y}$ and $\underline{y}$. The parameters μ^* and δ^* are optimal in the sense that the resulting controller (3) reduces the magnitude of the input oscillations to a minimum, compared to a conventional on-off controller.

In the following we assume an initial controller with $\mu = 0.5(\underline{u}+\overline{u})$, $\delta = \overline{u}-\mu$ that has completed one control cycle as depicted in Fig. 2. The control cycle starts at a time t_0 with

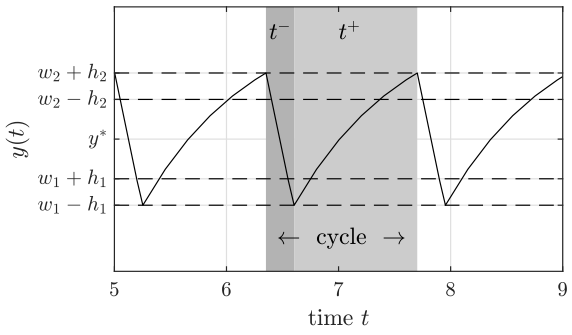

Fig. 2. One control cycle (highlighted in gray) with timespans t^- and t^+.

$y(t_0) = w_2 + h_2$, so that $s_1(t_0) = s_2(t_0) = 1$. The initial controller (3) operates like a conventional on-off controller and applies $u(t) = \mu - \delta = \underline{u}$ to the plant, therefore $y(t)$ decreases until $y(t_0 + t^-) = w_1 - h_1$ is reached. Since then $s_1(t_0 + t^-) = s_2(t_0 + t^-) = 0$, the controller applies $u(t) = \mu + \delta = \overline{u}$ and $y(t)$ increases until $y(t_0 + t^- + t^+)$ is reached and the cycle is completed. Let $\tau^- = t_0 + t^-$ and $\tau^+ = t_0 + t^- + t^+$ for better readability. By logging the switching instances of the binary sensors, the timespans t^+ and t^- can easily be measured by the controller.

3.1 Computation of μ^*

The computation of μ^* is iterative. We therefore first introduce a suboptimal $\tilde{u}$ that is computed from the current controller parameters and the measured timespans:

$$\tilde{\mu} = \frac{(\mu - \delta)t^- + (\mu + \delta)t^+}{t^+ + t^-} \; . \tag{4}$$

Proposition 1. Applying $u(t) = \tilde{\mu}$ to the undisturbed plant (1) yields $\tilde{y} \in [\underline{y}, \overline{y}]$ in steady state.

Proof. The desired $\tilde{y} \in [\underline{y}, \overline{y}]$ is given by the mean value of $y(t)$ from the completed cycle

$$\tilde{y} = \frac{\int_{t_0}^{\tau^-} y(t) \; \mathrm{d}t + \int_{\tau^-}^{\tau^+} y(t) \; \mathrm{d}t}{t^+ + t^-} \; , \tag{5}$$

since the first order model (1) does not exceed the limits $\underline{y}$ and $\overline{y}$. Solving (1) for $y(t)$ and substituting in (5) yields

$$\tilde{y} = \frac{\int_{t_0}^{\tau^-} ku(t) \; \mathrm{d}t + \int_{\tau^-}^{\tau^+} ku(t) \; \mathrm{d}t - [Ty(t)]_{t_0}^{\tau^-} - [Ty(t)]_{\tau^-}^{\tau^+}}{t^+ + t^-} \; . \tag{6}$$

Since $[Ty(t)]_{t_0}^{\tau^-} = TH$, $[Ty(t)]_{\tau^-}^{\tau^+} = -TH$, $u(t) = \mu - \delta = \text{const.}$ for $t \in [t_0, \tau^-)$ and $u(t) = \mu + \delta = \text{const.}$ for $t \in [\tau^-, \tau^+)$, (6) can be simplified to

$$\tilde{y} = \frac{k(\mu - \delta)t^- + k(\mu + \delta)t^+}{t^+ + t^-} \; . \tag{7}$$

Since $\tilde{y} = k\tilde{\mu}$ in steady state, (4) results from dividing (7) by k.

The timespans t^+ and t^- are measured by the controller and the parameters μ and δ required to evaluate (4) are the current, hence known controller parameters.

Proposition 2. $\tilde{\mu} \to \mu^*$ by repeated evaluation of (4) in subsequent control cycles.

Proof. Assume a disturbed $\tilde{\mu}_i = \mu^* + d$ with $\mu^* = 0$ and $d > 0$ in the current control cycle i. The disturbance decays when $0 < \left|\frac{\tilde{\mu}_{i+1}}{\tilde{\mu}_i}\right| < 1$, where $\tilde{\mu}_{i+1}$ results from (4) evaluated using $\tilde{\mu}_i$. Without loss of generality we choose $k = T = 1$ and $\underline{y} = -1$, $\overline{y} = 1$. With (4), $\left|\frac{\tilde{\mu}_{i+1}}{\tilde{\mu}_i}\right|$ becomes

$$\left|\frac{\tilde{\mu}_{i+1}}{\tilde{\mu}_i}\right| = \left|\frac{(t^+ + t^-)\cdot\tilde{\mu}_i + (t^+ - t^-)\cdot\delta}{(t^+ + t^-)\cdot\tilde{\mu}_i}\right| . \tag{8}$$

With $t^+ = -\log\left(\frac{(\tilde{\mu}_i+\delta)-\overline{y}}{(\tilde{\mu}_i+\delta)-\underline{y}}\right)$ and $t^- = -\log\left(\frac{(\tilde{\mu}_i-\delta)-\underline{y}}{(\tilde{\mu}_i-\delta)-\overline{y}}\right)$, (8) satisfies the criterion $0 < \left|\frac{\tilde{\mu}_{i+1}}{\tilde{\mu}_i}\right| < 1$ over the feasible parameter range $d \in (0, 1)$. Fig. 3 shows (8) evaluated over the feasible parameter range. The proof extends to any feasible parameter combination and holds analogously for a case where $\mu < \mu^*$.

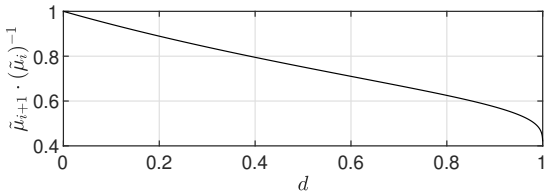

Fig. 3. Eqn. (8) evaluated over $d \in (0, 1)$.

3.2 Computation of δ^*

The minimal amplitude δ^* directly results from the steady state gain k of (1) and the hysteresis span H:

Proposition 3. The minimal amplitude δ^* is given by

$$\delta^* = \frac{H}{k} . \tag{9}$$

Proof. Applying $u(t) = \mu^*$ to (1) yields a steady state $y(t) = y^* = 0.5(\underline{y} + \overline{y})$, therefore applying $u(t) = \mu^* + \delta^* = \mu^* + \frac{0.5H}{k}$ yields a steady state $y(t) = \overline{y}$ and therefore guarantees switching. The same holds for the opposite case with the lower switching point $\underline{y}$.

A direct use of prop. 3 is impossible since we considered the parameters k and H to be unknown, but the simple structure of (1) can be exploited to compute δ^*. Assume that μ^* has been found as described in section 3.1 and yields $y(t) = y^*$ with $u(t) = \mu^*$, therefore one can simplify the following equations by assuming $y^* = \mu^* = 0$ without restriction. Let the controller have performed two consecutive control cycles with plant responses $y_1(t)$ and $y_2(t)$ resulting from control actions $u(t) = \delta_1$ and $u(t) = \delta_2$, respectively, with $\delta_2 < \delta_1$. δ_1 can be the initial δ or any previously used one, while δ_2 has to be chosen. We comment on the choice of δ_2 in section 3.3. Both plant responses start at $y_1(t = 0) = y_2(t = 0) = -0.5H$ and end at $y_1(t = t_1^+) = 0.5H$ and $y_2(t = t_2^+) = 0.5H$, with $t_1^+ < t_2^+$. Solving (1) for $y(t)$ with $u(t) = \delta$ yields

$$y(t) = e^{\frac{-t}{T}} y(t = 0) - \delta k \left(1 - e^{\frac{-t}{T}}\right) , \tag{10}$$

where k, T and $y(t = 0) = -0.5H$ are unknown. After adding $0.5H$ to both sides of (10), $y(t = 0)$ vanishes and (10) becomes

$$y(t) + 0.5H = \left(\delta + \frac{0.5H}{k}\right) \cdot k \cdot \left(e^{\frac{-t}{T}} - 1\right) . \tag{11}$$

By substituting t_1^+ and t_2^+ into (11), two equations with equal left hand side $y(t_1^+) + 0.5H = y(t_2^+) + 0.5H = H$ result. Rearranging then cancels H and

$$\frac{\delta_1\left(e^{\frac{-t_1^+}{T}} - 1\right)}{e^{\frac{-t_1^+}{T}} + 1} = \frac{\delta_2\left(e^{\frac{-t_2^+}{T}} - 1\right)}{e^{\frac{-t_2^+}{T}} + 1} \tag{12}$$

results. Solving (12) numerically for T yields the first unknown model parameter. With known T, (11) can be rearranged to

$$\left(e^{\frac{-t_1^+}{T}} - 1\right)\frac{k\delta_1}{0.5H} + e^{\frac{-t_1^+}{T}} = \left(e^{\frac{-t_2^+}{T}} - 1\right)\frac{k\delta_2}{0.5H} + e^{\frac{-t_2^+}{T}} , \tag{13}$$

which can be solved for $\frac{k}{0.5H}$. The inverse of $\frac{k}{0.5H}$ equals δ^* according to prop. 3. The predicted timespan t_p for the next control cycle (with $\delta = \delta^*$ and μ^*) is found by solving

$$\left(e^{\frac{-t_1^+}{T}} - 1\right)\frac{k\delta_1}{0.5H} + e^{\frac{-t_1^+}{T}} = \left(e^{\frac{-t_\mathrm{p}}{T}} - 1\right)\frac{k\delta^*}{0.5H} + e^{\frac{-t_p}{T}} \tag{14}$$

numerically for t_p with now known parameters $\frac{k}{0.5H}$ and T.

3.3 Considerations on the practical implementation

Due to the aperiodic first order behaviour of the plant (1), the timespans to reach $\underline{y}$ or $\overline{y}$ when applying $\mu^* \pm \delta^*$ may become infinite and therefore impracticable for a real world application. A relaxation of optimality is required, e.g. by applying $\kappa\delta^*$ with $\kappa > 1$ instead of δ^* to the plant. We chose $\kappa = 1.05$ for the experimental validation in section 5, thus added 5% to the computed optimal δ^*.

Measuring $y_2(t)$ requires a reduced $\delta_2 < \delta_1$. Using

$$\delta_2 = \rho\delta_1 \text{ with } 0 < \rho < 1 \tag{15}$$

with $\rho = 0.8$ is appropriate for most applications in our experience. However, if the plant gain k is small, ρ may have to be chosen larger to prevent δ_2 being lower than the optimal δ^* (which has not been identified at this point). Strong process noise or a very high process gain k may, on the other hand, require a smaller ρ to improve the signal to noise ratio for the measured times t_1^+ and t_2^+.

The proposed settings for κ and ρ proved successful in different laboratory applications.

4. AUTONOMOUS PARAMETER IDENTIFICATION

The proposed controller shall perform all the required steps to determine the controller parameters μ^* and δ^* without user interaction. The controller algorithm is divided into two phases: An initial self-learning phase spans

over the minimal number of control cycles required to collect all required information to determine μ^* and δ^*. The self-learning phase is followed by a constant output phase, where the plant is controlled with constant controller output $u(t) = \mu^*$. When $y(t)$ leaves the hysteresis range $[\underline{y}, \overline{y}]$ during the constant output phase, e.g. due to disturbances, the controller performs a disturbance rejection and restarts an adapted self-learning phase. The two phases and the disturbance rejection are outlined in the following.

4.1 Self-learning phase

The self-learning phase requires a total of $n+2$ consecutive control cycles, where n cycles are used for the iterative computation of μ^* (cf. Sec. 3.1) and two additional cycles are required for the computation of δ^*. Every cycle starts at $y(t_0) = w_2 + h_2$, reaches $y(t_0 + t^-) = w_1 - h_1$ and ends at $y(t_0 + t^- + t^+) = y(t_0) = w_2 + h_2$ as given in Fig. 2. The controller parameters μ, δ and γ are kept constant during any control cycle and the controller output is always given by (3).

Cycle 0: Initialization. The initial control cycle is activated at power-up or reset of the controller. The state of the plant is unknown at this moment, so $y(t = 0)$ may be located above, below or inside the hysteresis range. The initial cycle may therefore be incomplete, e.g. when $y(t = 0) < \underline{y}$, only the rising part of the cycle is performed. Initial parameters μ_0 and δ_0 are chosen so that $u(t) = \mu_0 \pm \delta_0$ spans the whole actuator range $[\underline{u}, \overline{u}]$. The parameter γ is 1 during the whole self-learning phase and the initial controller output is $u(t = 0) = \mu_0 - \delta_0$, which leads to a descending initial trajectory $y(t)$ until $y(t) = w_1 - h_1$ is reached. The controller (3) then switches to $u(t) = \mu_0 + \delta_0$, thus $y(t)$ rises until $y(t) = w_2 + h_2$ is reached, which marks the end of the initial cycle. The parameters μ_0 and δ_0 are kept unchanged, since, due to the unknown starting point $y(t = 0)$, the possibly incomplete initial cycle is not suited to perform the computations outlined in section 3.

Cycles 1 to n: Computation of μ^*. The following n control cycles iteratively compute $\tilde{\mu}$ by evaluating (4) at the end of every cycle. Convergence of of $\tilde{\mu}$ to μ^* has been reached when the time intervals t^+ and t^- are equal, which is the stopping criterion for the iteration and marks cycle n.

A valid output signal range, i.e. $u(t) = \tilde{\mu} \pm \delta \in [\underline{u}, \overline{u}]$, is guaranteed by applying

$$\delta := \delta + \min\left(\tilde{\mu} - \delta - \underline{u},\ \overline{u} - \tilde{\mu} - \delta,\ 0\right) \tag{16}$$

after evaluating (4). The mean timespan $t_\mathrm{m} = 0.5(t^+ + t^-)$ is computed at the end of every cycle and will be used for the disturbance rejection (cf. Sec. 4.3).

Cycles $n+1$ and $n+2$: Computation of δ^*. Cycle $n+1$ is performed with the previously computed μ^* and is required to measure the timespan $t_1^+ = t^+$ as required for the computation of δ^* by (12) and (13). All parameters are kept constant in cycle $n+1$.

Cycle $n+2$ is required to measure t_2^+ and is therefore applied with a reduced δ_2 as given by (15). At the end of cycle $n+2$, δ^* is computed by (12) and (13) and the predicted timespan t_p is computed by (14). In addition, μ^* is computed one additional time by (4) to incorporate a possible plant-model mismatch. With the end of cycle $n+2$ the self-learning phase is completed and the controller algorithm proceeds with the constant output phase.

4.2 Constant output phase

The last control cycle $n+2$ from the previous self-learning phase ended when $y(t)$ reached $w_2 + h_2$. The controller now applies $u(t) = \mu^* - \delta^*$ for half the predicted timespan, i.e. $0.5t_\mathrm{p}$, to achieve $y(t) = y^*$. Since t_p is the timespan required for $y(t)$ to travel from $w_2 + h_2$ to $w_1 - h_1$ with $u(t) = \mu^* - \delta^*$, $y(t)$ will equal y^* after $0.5t_\mathrm{p}$. After the timespan of $0.5t_\mathrm{p}$ has elapsed, the controller switches to a constant output $u(t) = \mu^*$ by setting $\gamma = 0$ in order to keep $y(t) = y^*$. As long as disturbances remain small enough, $y(t)$ will remain inside of the hysteresis range $[\underline{y}, \overline{y}]$ and the controller output $u(t) = \mu^*$ remains constant. The disturbance rejection is triggered by $y(t)$ leaving $[\underline{y}, \overline{y}]$ and will be outlined in the following.

4.3 Disturbance rejection during the self-learning phase

Disturbances arise due to varying parameters $k(t)$ and $z(t)$ of the model (1). Since we assumed that the plant is controllable by a conventional on-off controller (i.e. $\underline{y}$ and $\overline{y}$ can always be reached by applying inputs within $[\underline{u}, \overline{u}]$), the initial controller with μ_0 and δ_0 is able to control the plant, regardless of the disturbances. Since μ and δ are adjusted during the self-learning phase, $u(t)$ is now possibly constrained to a subset of $[\underline{u}, \overline{u}]$. Varying parameters $k(t)$ and $z(t)$ may therefore lead to a failing control as $y(t)$ may not reach the sensor switching points $\underline{y}$ or $\overline{y}$ any more and thus the self-learning algorithm is unable to proceed. The controller therefore monitors the timespans t^+ and t^- during cycles 1 to $n+2$ and compares the timespans to the mean timespan t_m from the previous cycle. A significantly increased timespan, e.g. $t^{+/-} > 2t_\mathrm{m}$, indicates that disturbances may have occured. The controller resets itself in this case and restarts the self-learning phase in cycle 0 with the initial parameters μ_0 and δ_0, to reject the disturbance.

4.4 Disturbance rejection during the constant output phase

During the constant output phase, a change in $k(t)$ or $z(t)$ may lead to $y(t)$ leaving the hysteresis area $[\underline{y}, \overline{y}]$, which is detected by a switching of one of the binary sensors, i.e. $s_1(t) = 0$ or $s_2(t) = 1$. Three causes for this disturbance will be distinguished in the following as they lead to different rejection methods. We note here that cause 3 is the most common, however, we included the other causes as they may be valuable for specific applications.

Cause 1: $z(t)$ changed. If only $z(t)$ changed and $k(t)$ remains constant, μ^* is updated using the current μ by

$$\mu^* = \begin{cases} \mu + \delta^* \ , & s_1(t) = 0 \\ \mu - \delta^* \ , & s_2(t) = 1 \end{cases} . \tag{17}$$

Since $k\delta^* = 0.5H$, adding δ^* to μ^* when $s_1(t) = 0$ will reject the disturbance as $y(t) = \underline{y} + 0.5H = y^*$. The case $y(t) > \overline{y}$, i.e. $s_2(t) = 1$, is treated analogously.

Cause 2: $k(t)$ changed. If only $k(t)$ changed and $z(t)$ remains constant, both μ^* and δ^* have to be adjusted. Let the steady state be $y(t) = y^* = k\mu^*$ for the original k and $y(t) = y^* \pm 0.5H = \tilde{k}\mu^*$ for the disturbed $k = \tilde{k}$, so that $y(t)$ has left the hysteresis range and $s_2 = 1$ or $s_1 = 0$, respectively. Equating both cases leads to

$$k\mu^* = \tilde{k}\mu^* \mp 0.5H \ . \tag{18}$$

Dividing both sides of (18) by $0.5H$ and μ^* yields

$$\frac{k}{0.5H} = \frac{\tilde{k}}{0.5H} \mp \frac{1}{\mu^*} \ . \tag{19}$$

As $\frac{\tilde{k}}{0.5H} = \tilde{\delta}^*$ is the new optimal input amplitude for the disturbed case as by (9), rearranging (19) yields

$$\tilde{\delta}^* = \begin{cases} \left(\frac{1}{\delta^*} + \frac{1}{\mu^*}\right)^{-1}, & s_1(t) = 0 \\ \left(\frac{1}{\delta^*} - \frac{1}{\mu^*}\right)^{-1}, & s_2(t) = 1 \end{cases} \ . \tag{20}$$

Finally, μ^* is corrected by applying (17). The controller then uses $\tilde{\delta}^*$ as the new optimal amplitude δ^*.

Cause 3: Both $k(t)$ and $z(t)$ changed. If both $k(t)$ and $z(t)$ have changed, a restart of the controller with the self-learning phase is the only way to reject the disturbance. However, instead of resetting the controller to the initial parameters μ_0 and δ_0, the above considerations can be exploited to achieve a less aggressive control. We choose to reset the controller parameters to $\mu = \mu^*$ by (17) and $\delta = \tilde{\delta}^*$ by (20), however, prevent a lower δ than the one that was used before the disturbance occured. The controller then restarts with the self-learning phase in cycle 0.

5. RESULTS

We evaluated the proposed controller in a laboratory test setup reflecting the sample process from Fig. 1. A standard centrifugal pump delivers fluid into a storage tank, the rotational speed of the pump is the process input $u(t)$ and can be used to adjust the flow into the storage tank. $u(t)$ is an analog signal with $u(t) \in [0\text{V}, 10\text{V}]$. A variable outflow from the storage tank was used to simulate disturbances. The fluid level in the storage tank is the controlled process variable $y(t)$. The level is measured by a dedicated sensor and is available as a continuous measurement. We use the continuous measurement to simulate two binary sensors by applying (2) on $y(t)$ to generate $s_1(t)$ and $s_2(t)$ with $w_1 = 217.5$ mm, $w_2 = 247.5$ mm and $h_1 = h_2 = 2.5$ mm, respectively.

The adaptive binary controller was implemented in Matlab / Simulink on a standard PC. An I/O-card was used to communicate with the hydraulic process. Figure 4 depicts the results from a measurement run over 50 minutes. The upper diagram shows the fluid level $y(t)$ together with the two binary sensor switching levels. The middle diagram shows the corresponding binary sensor signals $s_1(t)$ and $s_2(t)$. The lower diagram shows the controller output $u(t)$ and the parameters $\mu(t)$ and $\delta(t)$ evolving over time.

The control starts with the initialization in cycle 0 with the initial paramaters $\mu_0 = \delta_0 = 5\text{V}$, thus applies $u(t) = \mu_0 + \delta_0 = 10\text{V}$ to the plant until $y(t) = w_2 + h_2$ is reached. The

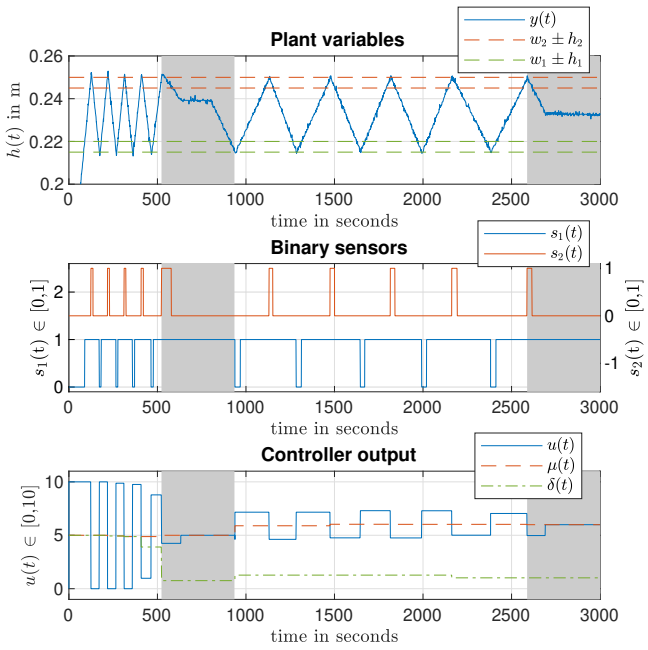

Fig. 4. Control performance of the proposed control in the laboratory test setup. The gray areas highlight the constant output phase.

subsequent iteration of μ^* requires only $n = 2$ cycles until symmetry is achieved and $t^- \approx t^+$. The two cycles result in only marginal changes to μ, as the initial value of $\mu = 5$ is incidentally a good choice for the process in the current configuration. At the end of cycle $n + 1 = 3$ at about 400 seconds, δ is reduced for the first time by applying (15). At the end of cycle $n + 2 = 4$ at about 500 seconds, the optimal parameters δ^*, μ^*, and the predicted timespan t_p are computed. The controller then enters the constant output phase and applies $u(t) = \mu^* - \delta^*$ for $0.5t_\text{p} \approx 100$ seconds, and then $u(t) = \mu^*$ by setting $\gamma = 0$. The constant output phase is highlighted by a gray area in Fig. 4. The controlled variable $y(t)$ settles at a constant value, though with a slight offset to y^*, which is caused by the plant model mismatch.

At about 800 seconds, the outflow from the storage tank is increased to simulate a disturbance, resulting in a decrease of $y(t)$. The controller initiates the disturbance rejection at about 900 seconds after detecting $s_1(t) = 0$ and computes δ and μ as new initial parameters for the restart of the self-learning phase. Evidently, the prediction of the new parameters μ and δ as described in section 4.4 (cause 3) yields proper results, so that both parameters do not change significantly during the following self-learning phase. The self-learning is performed with significantly reduced input amplitude, compared to the initial control. At about 2600 seconds, the constant output phase is initiated again and $y(t)$ settles close to y^*. The control then runs with constant $u(t)$ and nearly constant $y(t)$ until the end of the measurement.

We analyzed the energy demand of the proposed adaptive binary control and compared it to a conventional PID control and a simple on-off control. The results are depicted in Figure 5 and originate from the same measurement run

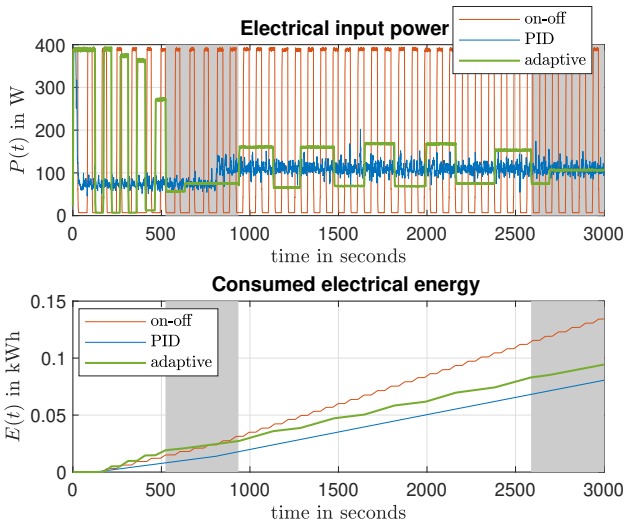

Fig. 5. Comparison of power demand and accumulated energy consumption for the adaptive binary controller and two established control implementations. The gray areas highlight the constant output phase of the adaptive controller.

already shown in Figure 4. The upper diagram in Fig. 5 shows the electrical power demand $P(t)$, while the lower diagram shows the accumulated energy consumption $E(t)$ over time for all three control variants.

The PID controller serves as a benchmark here, as the energy consumption is the lowest of all three variants. However, the PID controller requires a continuous measurement of $y(t)$ and thus a more complex and expensive sensor, in contrast to the two other methods that only require simple float switches. As anticipated, the simple on-off control is the least energy-efficient variant, due to the repeated acceleration of the pump to full speed. The adaptive binary controller performs like the simple on-off controller during its initial self-learning phase. However, after completing the self-learning, the adaptive controller provides a constant pump speed, comparable to the benchmark PID control. The repeated self-learning after the disturbance at about 800 seconds also shows an only marginally increased energy demand compared to the PID control. During the constant output phases, the energy demands of adaptive binary control and PID control are nearly equal and significantly lower than for the simple on-off control. At the end of the 50 minute measurement, the on-off control required 0.134 kWh, the adaptive control reduced the energy consumption to 70%, and the PID control to 60%, relative to the on-off control. Extended constant output phases will further reduce the energy consumption of the adaptive controller.

6. CONCLUSION

We proposed a self-learning binary controller for plants with two binary measurements. The controller combines the benefits of a conventional on-off control in terms of simplicity for the user with the benefits of a continuous control in terms of energy consumption and control quality. We showed that a significant reduction in the energy consumption of the plant can be achieved by replacing a simple on-off controller with the proposed adaptive controller, while no further expenses regarding sensor hardware and controller tuning arise.

In further works we will implement the controller on an industrial hardware and perform more elaborate field tests to further refine the algorithm. Also an extension of the control concept to a wider system class is subject to current research.

ACKNOWLEDGEMENTS

Funding by the Deutsche Bundesstiftung Umwelt is gratefully acknowledged.

REFERENCES

A. Afram and F. Janabi-Sharifi. Effects of dead-band and set-point settings of on/off controllers on the energy consumption and equipment switching frequency of a residential HVAC system. *Journal of Process Control*, volume 47, pages 161-174, 2016.

H. Ahmad and U. Atikol. A simple algorithm for reducing the operation frequency of residential water pumps during peak hours of power consumption. *Energy Science and Engineering*, volume 6.4, pages 253-271, 2019.

K. J. Åström. Oscillations in systems with relay feedback. *Adaptive Control, Filtering, and Signal Processing*, Springer, New York, 1995.

M. Bek and B. Dietzel. Digital two step controller for an actuator element. European Patent EP0894293B1, April 19, 1996.

K. S. Cetin, M. H. Fathollahzadeh, N. Kunwar, H. Do, and P. C. Tabares-Velasco. Development and validation of an HVAC on/off controller in EnergyPlus for energy simulation of residential and small commercial buildings. *Energy and Buildings*, volume 183, pages 467-483, 2019.

T. Co. Relay-Stabilization and Bifurcations of Unstable SISO Processes With Time Delay. *IEEE Transactions on Automatic Control*, volume 55, no. 5, pages 1131–1141, 2010.

A. Colombo, M. di Bernardo, S. J. Hogan and P. Kowalczyk. Complex Dynamics in a Hysteretic Relay Feedback System with Delay. *Journal of Nonlinear Science*, volume 17, pages 85–108, 2007.

J. M. Goncalves, A. Megretski, and M. A. Dahleh. Global stability of relay feedback systems. *IEEE Transactions on Automatic Control*, volume 46, issue 4, pages 550–562, 2001.

J. M. Goncalves, A. Megretski, and M. A. Dahleh. Global analysis of piecewise linear systems using impact maps and surface Lyapunov functions. *IEEE Transactions on Automatic Control*, volume 48, issue 12, pages 2089–2106, 2003.

L. Hetel, E. Fridman, and T. Floquet. Variable structure control with generalized relays: A simple convex optimization approach. *IEEE Transactions on Automatic Control*, volume 60, no. 2, pages 497–502, 2015.

S. Leonow and M. Mönnigmann. A self-learning binary controller for increased control performance. *Proceedings of the 18th European control conference (ECC)*, pages 3621-3637, 2019.

S. Leonow, T. Gunder and M. Mönnigmann. A self-learning binary controller for energy efficient pump operation. *Proceedings of the 4th International Rotating Equipment Conference (IREC)*, 2019.

Y. E. Yoon and E. N. Johnson. Analysis of Simple Relay Feedback Adaptive Control. *AIAA Guidance, Navigation, and Control Conference, AIAA SciTech Forum*, 2017.